2015/04/16
Head Id: 284702
Archive Id: 284790P
Archive Date: 2015/04/15
Archive Tag: trunk

Search for quark contact interactions and extra spatial dimensions using dijet angular distributions in proton-proton collisions at $\sqrt{s} = 8$ TeV

The CMS Collaboration

Abstract

A search is presented for quark contact interactions and extra spatial dimensions in proton-proton collisions at $\sqrt{s} = 8$ TeV using dijet angular distributions. The search is based on a data set corresponding to an integrated luminosity of 19.7 fb^{-1} collected by the CMS detector at the CERN LHC. Dijet angular distributions are found to be in agreement with the perturbative QCD predictions that include electroweak corrections. Limits on the contact interaction scale from a variety of models at next-to-leading order in QCD corrections are obtained. A benchmark model in which only left-handed quarks participate is excluded up to a scale of 9.0 (11.7) TeV for destructive (constructive) interference at 95% confidence level. Lower limits between 5.9 and 8.4 TeV on the scale of virtual graviton exchange are extracted for the Arkani-Hamed–Dimopoulos–Dvali model of extra spatial dimensions.

1 Introduction

High momentum-transfer proton-proton collisions at the CERN LHC probe the dynamics of the underlying interaction at distances below 10^{-19} m. Often these collisions produce a pair of jets (dijets) approximately balanced in transverse momentum p_{T}. These dijet events provide an ideal testing ground to probe the validity of perturbative quantum chromodynamics and to search for new phenomena such as quark compositeness or additional, compactified spatial dimensions. A particularly suitable observable for this purpose is the dijet angular distribution [1] expressed in terms of $\chi_{\mathrm{dijet}} = \exp(|y_1 - y_2|)$, where y_1 and y_2 are the rapidities of the two jets with the highest transverse momenta. Rapidity is defined as $y = \ln\left[(E + p_z) / (E - p_z)\right]/2$ with E being the jet energy and p_z the projection of the jet momentum onto the beam axis. For the scattering of massless partons, χ_{dijet} is related to the polar scattering angle θ^* in the partonic center-of-mass (c.m.) frame by $\chi_{\mathrm{dijet}} = (1 + |\cos\theta^*|)/(1 - |\cos\theta^*|)$. The choice of the variable χ_{dijet} is motivated by the fact that for Rutherford scattering the angular distribution is approximately independent of χ_{dijet}. In perturbative QCD the dijet angular distribution at small c.m. scattering angles is approximately independent of the underlying partonic level process and exhibits behavior similar to Rutherford scattering, characteristic of spin-1 particle exchange. Signatures of new physics (NP), such as quark contact interactions (CI) or virtual exchange of Kaluza–Klein [2] excitations of the graviton, that exhibit angular distributions that are more isotropic than those predicted by QCD, could appear as an excess of events at low values of χ_{dijet}.

Models of quark compositeness [3–5] postulate interactions between quark constituents at a characteristic scale Λ that is much larger than the quark masses. At energies well below Λ, these interactions can be approximated by a CI characterized by a four-fermion coupling. The effective Lagrangian for flavor-diagonal color-singlet couplings between quarks can be written as [4, 5]:

$$\mathcal{L}_{\mathrm{qq}} = \frac{2\pi}{\Lambda^2}\left[\eta_{LL}(\bar{\mathrm{q}}_L\gamma^\mu \mathrm{q}_L)(\bar{\mathrm{q}}_L\gamma_\mu \mathrm{q}_L) + \eta_{RR}(\bar{\mathrm{q}}_R\gamma^\mu \mathrm{q}_R)(\bar{\mathrm{q}}_R\gamma_\mu \mathrm{q}_R) + 2\eta_{RL}(\bar{\mathrm{q}}_R\gamma^\mu \mathrm{q}_R)(\bar{\mathrm{q}}_L\gamma_\mu \mathrm{q}_L)\right],$$

where the subscripts L and R refer to the left and right chiral projections of the quark fields respectively and η_{LL}, η_{RR}, and η_{RL} are taken to be 0, $+1$, or -1. The various combinations of $(\eta_{LL}, \eta_{RR}, \eta_{RL})$ correspond to different CI models. The following CI scenarios with color-singlet couplings between quarks are investigated:

Λ	$(\eta_{LL}, \eta_{RR}, \eta_{RL})$
$\Lambda^{\pm}_{LL}$	$(\pm 1, \ 0, \ 0)$
$\Lambda^{\pm}_{RR}$	$(\ 0, \pm 1, \ 0)$
$\Lambda^{\pm}_{VV}$	$(\pm 1, \pm 1, \pm 1)$
$\Lambda^{\pm}_{AA}$	$(\pm 1, \pm 1, \mp 1)$
$\Lambda^{\pm}_{(V-A)}$	$(\ 0, \ 0, \pm 1)$

Note that the models with positive (negative) η_{LL} or η_{RR} lead to destructive (constructive) interference with the QCD terms and a lower (higher) cross section in the limit of high partonic c.m. energies. In all CI models discussed in this Letter, next-to-leading-order (NLO) QCD corrections are employed to calculate the cross sections. In proton-proton collisions the $\Lambda^{\pm}_{LL}$ and $\Lambda^{\pm}_{RR}$ models result in identical tree-level cross sections and NLO corrections, and consequently lead to the same sensitivity. For $\Lambda^{\pm}_{VV}$ and $\Lambda^{\pm}_{AA}$, as well as for $\Lambda^{\pm}_{(V-A)}$, the CI predictions are identical at tree-level, but exhibit different NLO corrections and yield different sensitivity.

Measurements of dijet angular distributions at the Fermilab Tevatron have been reported by the CDF [6] and D0 [7, 8] Collaborations, and at the LHC by the CMS [9–11] and ATLAS [12, 13] Collaborations. The most stringent limits to date on CI models calculated at tree-level have been obtained by the CMS Collaboration from the inclusive jet p_{T} spectrum [14], which excludes $\Lambda^{+}_{LL} < 9.9\,\mathrm{TeV}$ and $\Lambda^{-}_{LL} < 14.3\,\mathrm{TeV}$. Constraints on CI models with NLO corrections have been previously obtained from a search in the dijet angular distributions [9], excluding in particular $\Lambda^{+}_{LL} < 7.5\,\mathrm{TeV}$ and $\Lambda^{-}_{LL} < 10.5\,\mathrm{TeV}$.

Dijet angular distributions are also sensitive to signatures from the Arkani-Hamed–Dimopoulos–Dvali (ADD) model [15, 16] of compactified extra dimensions (EDs) that provides a possible solution to the hierarchy problem of the standard model (SM). In the ADD model, gravity is assumed to propagate in the entire higher-dimensional space, while SM particles are confined to a (3+1) dimensional subspace. As a result, the fundamental Planck scale M_{D} in the ADD model is much smaller than the (3+1) dimensional Planck energy scale M_{Pl}, which may lead to phenomenological effects that can be tested with proton-proton collisions at the LHC. The coupling of the graviton in higher-dimensional space to the SM fields can be described by a (3+1)-dimensional tower of Kaluza–Klein (KK) graviton excitations, each coupled to the energy-momentum tensor of the SM field with gravitational strength. The effects of a virtual graviton exchange can therefore be approximated at leading-order (LO) by an effective (3+1)-dimensional theory that sums over KK excitations of a virtual graviton. This sum is divergent, and therefore has to be truncated at a certain energy scale of order M_{D}, where the effective theory is expected to break down. Such a theory predicts a non-resonant enhancement of dijet production, whose angular distribution differs from the QCD prediction. Two parameterizations for virtual graviton exchange in the ADD model are considered, namely the Giudice–Rattazzi–Wells (GRW) [17] and the Han–Lykken–Zhang (HLZ) [18] conventions. Though not considered in this paper, another convention by Hewett [19] exists. In the GRW convention the sum over the KK states is regulated by a single cutoff parameter Λ_T. The HLZ convention describes the effective theory in terms of two parameters, the cutoff scale M_S and the number of extra spatial dimensions n_{ED}. The parameters M_S and n_{ED} can be directly related to Λ_T [20]. We consider scenarios with 2 to 6 EDs. The case of $n_{\mathrm{ED}} = 1$ is not considered since it would require an ED of the size of the order of the solar system; the gravitational potential at these distances would be noticeably modified and this case is therefore excluded. The case of $n_{\mathrm{ED}} = 2$ is special in the sense that the relation between M_S and Λ_T also depends on the parton-parton c.m. energy $\sqrt{\hat{s}}$. Signatures from virtual graviton exchange have previously been sought in dilepton [21, 22], diphoton [23, 24], and dijet [7, 25, 26] final states, where the most stringent limits come from the dilepton searches and range from 3.5 to 4.9 TeV.

In this Letter, we extend previous searches for contact interactions to higher CI scales, for a wide range of models that include the exact NLO QCD corrections to dijet production. In addition, we explore various models of compactified extra dimensions. Using a data sample corresponding to an integrated luminosity of $19.7\,\mathrm{fb}^{-1}$ at $\sqrt{s} = 8\,\mathrm{TeV}$, the measured dijet angular distributions, unfolded for detector effects, are compared to QCD predictions at NLO, including for the first time electroweak (EW) corrections.

2 Event selection

A detailed description of the CMS detector, together with a definition of the coordinate systems used and the relevant kinematic variables, can be found in Ref. [27]. The central feature of the CMS apparatus is a superconducting solenoid of 6 m internal diameter, providing an axial field of 3.8 T. Within the solenoid are the silicon pixel and strip trackers, which cover the region

of pseudorapidity $|\eta| < 2.5$, and the lead tungstate crystal electromagnetic and the brass and scintillator hadronic calorimeters, which surround the tracking volume and cover $|\eta| < 3$. Muons are measured in gas-ionization detectors embedded in the steel flux-return yoke of the solenoid with a coverage of $|\eta| < 2.4$.

Events are reconstructed using a particle-flow technique [28, 29] which combines information from all CMS subdetectors to identify and reconstruct in an optimal way the individual particle candidates (charged hadrons, neutral hadrons, electrons, muons, and photons) in each event. These particle candidates are clustered into jets using the anti-k_T algorithm [30] as implemented in the FASTJET package [31] with a size parameter $R = 0.5$. Jet energy scale corrections [32] derived from data and Monte Carlo (MC) simulation are applied to account for the response function of the calorimeters for hadronic showers.

The CMS trigger system uses a two-tiered system comprising a level-1 trigger (L1) and a high-level trigger (HLT) to select physics events of interest for further analysis. The selection criteria used in this analysis are the inclusive single-jet triggers, which require one L1 jet and one HLT jet with various thresholds on the jet p_T, as well as trigger paths with thresholds on the dijet mass and scalar sum of the jet p_T. The p_T of jets is corrected for the response of the detector at both L1 and the HLT. The efficiency of each single-jet trigger is measured as a function of dijet mass M_{jj} using events selected by a lower-threshold trigger.

Events with at least two reconstructed jets are selected from an inclusive jet sample and the two highest-p_T jets are used to measure the dijet angular distributions for different ranges in M_{jj}. In units of TeV the M_{jj} ranges are (1.9, 2.4), (2.4, 3.0), (3.0, 3.6), (3.6, 4.2), and >4.2. The lowest M_{jj} range is chosen such that the trigger efficiency exceeds 99% in all bins of χ_{dijet} considered in this analysis. The two highest M_{jj} ranges were chosen to maximize the expected sensitivity to the new physics signals considered. Events with spurious jets from noise and noncollision backgrounds are rejected by applying loose quality criteria [33] to jet properties and requiring a reconstructed primary vertex within ± 24 cm of the detector center along the beam line and within 2 cm of the detector center in the plane transverse to the beam. The main primary vertex is defined as the one with the largest summed p_T^2 of its associated tracks. The phase space for this analysis is defined by selecting events with $\chi_{\text{dijet}} < 16$ and $y_{\text{boost}} < 1.11$, where $y_{\text{boost}} = \frac{1}{2}|y_1 + y_2|$. This choice of values restricts the two jets within $|y| < 2.5$. The highest value of M_{jj} observed in this data sample is 5.2 TeV.

3 Cross section unfolding and uncertainties

The measured χ_{dijet} distributions, defined as $(1/\sigma_{\text{dijet}})(\mathrm{d}\sigma_{\text{dijet}}/\mathrm{d}\chi_{\text{dijet}})$, are corrected for migration effects due to the finite jet energy and position resolutions of the detector. Fluctuations in the jet response cause event migrations in χ_{dijet} as well as in dijet mass. Therefore, a two-dimensional unfolding in these variables is performed using the D'Agostini method [34] as implemented in the ROOUNFOLD package [35]. The unfolding corrections are determined from a response matrix that maps the true M_{jj} and χ_{dijet} distributions onto the measured ones. This matrix is derived using particle-level jets from HERWIG++ version 2.5.0 [36, 37] with the tune of version 2.4. The jets are smeared in p_T with a double-sided Crystal-Ball parameterization [38] of the response, which takes into account the full jet energy response including non-Gaussian tails. The unfolding correction factors as a function of χ_{dijet} vary from less than 3% in the lowest M_{jj} range to less than 20% in the highest M_{jj} range.

The main experimental systematic uncertainties in this analysis are caused by the jet energy scale, the jet energy resolution, and the unfolding modeling and detector simulation. The over-

all jet energy scale uncertainty varies between 1% and 2% and has a dependence on pseudorapidity of less than 1% per unit of η [32]. The jet energy scale uncertainty is divided into 21 uncorrelated sources [39]. The effect of each source is propagated to the dijet angular distributions and then summed in quadrature to take into account uncorrelated p_T- and η-dependent sources that could cancel if varied simultaneously. The resulting uncertainty in the χ_{dijet} distributions due to the jet energy scale uncertainties is found to be less than 2.0% (2.6%) at low (high) M_{jj} over all χ_{dijet} bins, and the maximum uncertainty in a given M_{jj} bin is typically found to be in the lowest χ_{dijet} bin.

The jet energy resolution is known to within 10% of its value in the phase space considered in this analysis [32]. The systematic uncertainty in the χ_{dijet} distributions due to this effect was evaluated by varying the width of the Gaussian core of the Crystal-Ball parameterization of the response by $\pm$10% and comparing the resultant unfolding corrections before and after these changes. The resulting uncertainty in the χ_{dijet} distributions is 0.5% (1.5%) in the lowest (highest) M_{jj} range. In addition, a systematic uncertainty in the tails of the jet response function is evaluated by determining a correction factor using a Gaussian ansatz [32] rather than the double-sided Crystal-Ball (Gaussian with tails) function to parameterize the response. Since the Gaussian assumption corresponds to the extreme case of the complete absence of a tail, the associated uncertainty has been taken to be 50% of the difference between this correction and the nominal correction based on the Crystal-Ball function. This covers the uncertainty in the understanding of the tails from jet resolution tail measurements. The size of this uncertainty varies from less than 1% in the lowest M_{jj} range to less than 13% in the highest M_{jj} range.

A systematic uncertainty in the unfolding due to the use of a parameterized model of the jet p_T and position resolutions to determine the unfolding correction factors is estimated by comparing the smeared χ_{dijet} distributions to the ones from a detailed simulation of the CMS detector using GEANT4 [40]. This uncertainty is found to be less than 0.4% (5%) in the lowest (highest) M_{jj} range. A further systematic uncertainty in the unfolding for the modeling of the dijet spectra with HERWIG++ [0.1% (1.2%) in the lowest (highest) M_{jj} range], is estimated from a comparison of the unfolding corrections from HERWIG++ with those obtained from PYTHIA 8 version 8.165 [41] with tune 4C [42].

The uncertainty from additional interactions in the same proton bunch crossing as the interaction of interest, called pileup, is determined in simulation by varying the minimum bias cross section within its measured uncertainty of 6% [43]. No significant effect is observed. Though in the statistical analysis of the data the uncertainties are treated separately, for display in tables and figures, the total experimental systematic uncertainty in the χ_{dijet} distributions is calculated as the quadratic sum of the contributions due to the uncertainties in the jet energy calibration, jet p_T resolution, and unfolding correction. The total uncertainty including statistical uncertainties is less than 2.5% (49%) for the lowest (highest) M_{jj} range. Experimental uncertainties are evaluated for both the QCD background and signal predictions, however, the resulting uncertainties do not differ significantly.

4 Theoretical predictions

The normalized dijet angular distributions are compared to the predictions of perturbative QCD. The NLO calculation is provided by NLOJET++ version 4.1.3 [44, 45] within the FASTNLO framework version 2 [46, 47]. The factorization (μ_F) and renormalization (μ_R) scales are defined to be the average p_T of the two jets, $\langle p_{T1,2} \rangle$. Electroweak corrections for dijet production have been derived in Ref. [48], the authors of which provided us with the corresponding corrections for the χ_{dijet} distributions. These corrections change the predictions of the normalized χ_{dijet}

distributions by up to 4% (14%) at low (high) M_{jj}. Since fast re-evaluation techniques for different choices of PDFs or scales are not yet available for the electroweak correction part of the theory, the factors have been applied here without additional uncertainties. A figure showing these corrections can be found in the Appendix. The impact of non-perturbative effects such as hadronization and multiple parton interactions is estimated using PYTHIA 8 and HERWIG++. These effects are found to be negligible.

The dominant uncertainty in the QCD predictions is associated with the choice of the μ_R and μ_F scales and is evaluated following the proposal in Ref. [49] by varying the default choice of scales in the following six combinations: $(\mu_F/\langle p_{\mathrm{T1,2}}\rangle, \mu_R/\langle p_{\mathrm{T1,2}}\rangle) = (1/2, 1/2), (1/2, 1), (1,1/2), (2, 2), (2, 1)$, and $(1, 2)$. These scale variations change the QCD predictions of the normalized χ_{dijet} distributions by less than 9% (18%) at low (high) M_{jj}. The uncertainty due to the choice of parton distribution functions (PDF) is determined from the 22 uncertainty eigenvectors of CT10 [50] using the procedure described in Ref. [50], and is found to be less than 0.6% (1.0%) at low (high) M_{jj}. A summary of the systematic uncertainties in the theoretical predictions is given in Table 1 together with the experimental ones. In the highest M_{jj} range, the dominant experimental contribution is the statistical uncertainty while the dominant theoretical contribution is the QCD scale uncertainty.

Table 1: Summary of the experimental and theoretical uncertainties in the normalized χ_{dijet} distributions. For the lowest, second highest and highest M_{jj} ranges, the relative shift (in %) of the lowest χ_{dijet} bin from its nominal value is quoted. While in the statistical analysis each systematic uncertainty is represented by a change of the χ_{dijet} distribution correlated among all χ_{dijet} bins, this table summarizes each uncertainty by a representative number to demonstrate the relative contributions.

Uncertainty	$1.9 < M_{jj} < 2.4$ TeV (%)	$3.6 < M_{jj} < 4.2$ TeV (%)	$M_{jj} > 4.2$ TeV (%)
Statistical	1.0	2.3	47
Jet energy scale	2.0	2.1	2.5
Jet energy resolution (tails)	1.0	2.0	13
Jet energy resolution (core)	0.5	0.6	1.5
Unfolding, modeling	0.1	1.2	1.2
Unfolding, detector simulation	0.4	1.0	5.0
Pileup	<0.1	<0.1	<1.0
Total experimental	2.5	4.1	49
QCD NLO scale (6 variations of μ_R and μ_F)	$^{+9.0}_{-3.4}$	$^{+11}_{-4.0}$	$^{+18}_{-6.3}$
PDF (CT10 eigenvectors)	0.6	0.7	1.0
Non-perturbative effects	<1.0	<1.0	<0.2
Total theoretical	9	11	18

For calculating the CI terms as well as the interference between the CI terms and QCD terms at LO and NLO in QCD the CIJET program version 1.0 [51] has been employed. The CI models at LO are cross-checked with the implementation in PYTHIA 8 and found to be consistent. The ADD predictions are calculated with PYTHIA 8.

5 Results

In Fig. 1 the measured χ_{dijet} distributions, corrected for instrumental effects and normalized by their respective event counts, for all M_{jj} ranges, are compared to theoretical predictions. The

data are well described by NLO calculations that incorporate EW corrections. No significant deviation from the SM predictions is observed. The distributions are also compared to predictions for SM+CI with Λ^{+}_{LL} (NLO) $=$ 10 TeV and predictions for SM+ADD with Λ_T (GRW) $=$ 7 TeV.

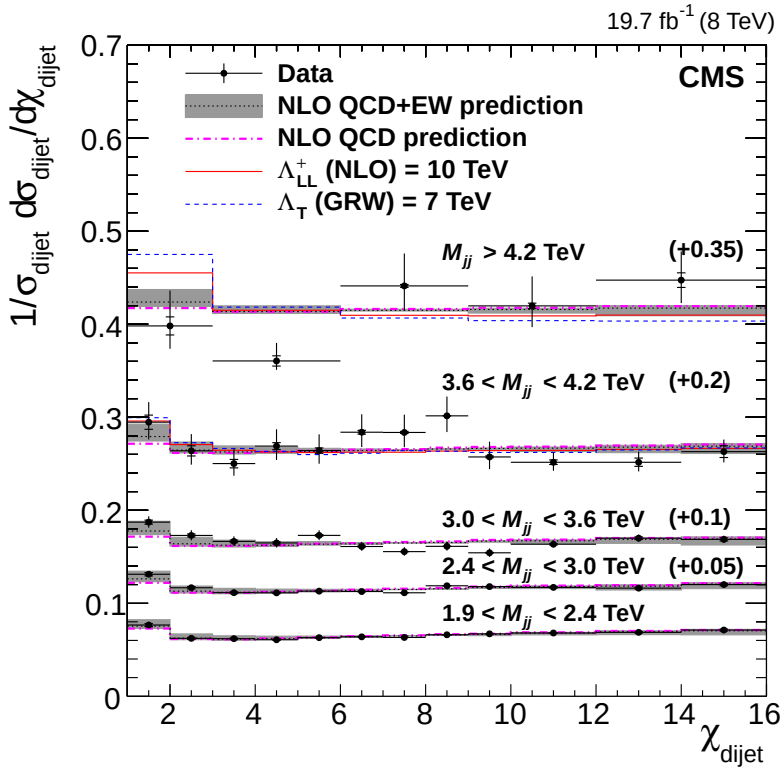

Figure 1: Normalized χ_{dijet} distributions for 19.7 fb^{-1} of integrated luminosity at $\sqrt{s} = 8$ TeV. The corrected data distributions are compared to NLO predictions with EW corrections (black dotted line). For clarity the individual distributions are shifted vertically by offsets indicated in parentheses. Theoretical uncertainties are indicated as a gray band. The error bars represent statistical and experimental systematic uncertainties combined in quadrature. The ticks on the error bars represent experimental systematic uncertainties only. The horizontal bars indicate the bin widths. The NLO QCD prediction without EW corrections is also shown (purple dashed dotted). The prediction for SM+CI with Λ^{+}_{LL} (NLO) $=$ 10 TeV is shown (red solid line), and so is the prediction for SM+ADD with Λ_T (GRW) $=$ 7 TeV (blue dashed line).

The measured χ_{dijet} distributions are used to determine exclusion limits on CI models that include full NLO QCD corrections to dijet production induced by contact interactions calculated with CIJET. Limits are also extracted for CI models calculated at LO with CIJET and ADD models implemented in PYTHIA 8. To take into account the NLO QCD and EW corrections in these LO models, the cross section difference $\sigma^{\text{QCD}}_{\text{NLO+EW corr}} - \sigma^{\text{QCD}}_{\text{LO}}$ is evaluated for each M_{jj} and χ_{dijet} bin and added to the PYTHIA 8 +ADD and LO QCD+CI predictions. With this procedure, an SM+CI (SM+ADD) prediction is obtained where the QCD terms are corrected to NLO with EW corrections while the CI (ADD) terms are calculated at LO. The variations due to theoretical uncertainties associated with scales and PDFs are applied only to the QCD terms of the prediction, thereby treating the effective new physics terms as fixed benchmark terms.

In Fig. 2, the χ_{dijet} distributions for the two highest M_{jj} ranges are compared to various CI and ADD models. Only the two highest M_{jj} ranges are used to determine limits of CI and ADD

model parameters since the added sensitivity from the lower M_{jj} ranges is negligible.

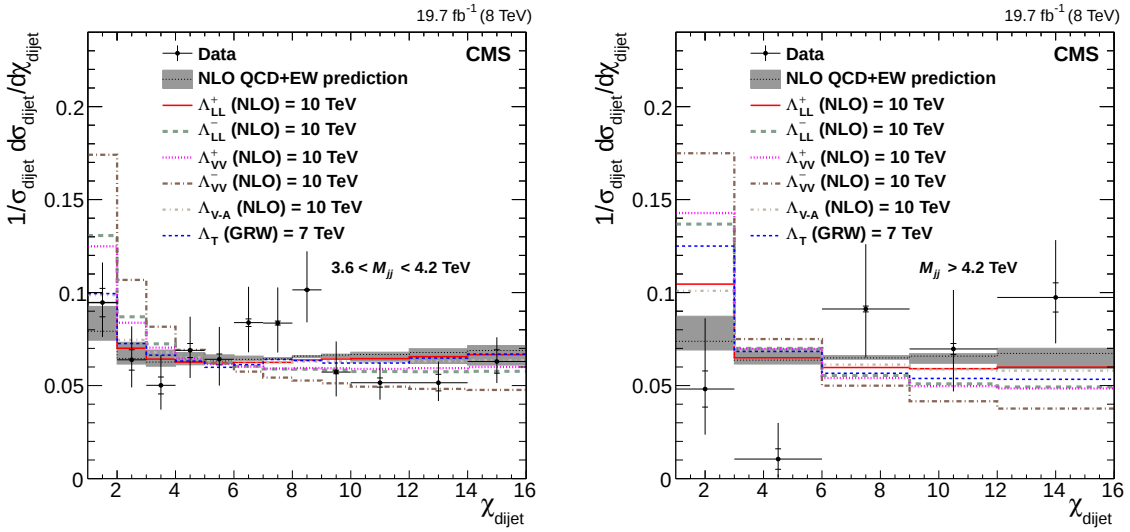

Figure 2: Normalized χ_{dijet} distributions in the two highest M_{jj} ranges. The corrected data distributions are compared to NLO predictions with EW corrections (black dotted line). Theoretical uncertainties are indicated as gray bands. The error bars represent statistical and experimental systematic uncertainties combined in quadrature. The ticks on the error bars represent experimental systematic uncertainties only. The horizontal bars indicate the bin widths. The predictions for the various CI and ADD models are overlaid.

We quantify the significance of a NP signal with respect to the SM-only hypothesis by means of the likelihood for the SM-only, L_{SM}, and the likelihood for the SM with new physics, $L_{\text{SM+NP}}$. The L_{SM} and $L_{\text{SM+NP}}$ are defined as products of Poisson likelihood functions for each bin in χ_{dijet} for the two highest ranges of M_{jj}. The predictions for each M_{jj} range are normalized to the number of observed events in that range. The p-values for the two hypotheses, $p_{\text{SM+NP}}(q \geq q_{\text{obs}})$ and $p_{\text{SM}}(q \leq q_{\text{obs}})$, are based on the log-likelihood ratio $q = -2\ln(L_{\text{SM+NP}}/L_{\text{SM}})$. They are evaluated from ensembles of pseudo-experiments, in which systematic uncertainties are taken into account via nuisance parameters which affect the χ_{dijet} distribution, varied within their Gaussian uncertainties when generating the distributions of q [52].

We note that there is an observed difference between the NLO QCD calculations with EW corrections and the NLO QCD-only hypothesis in the above defined likelihood ratio, which corresponds to a significance of 1.1 standard deviation.

The agreement of the data with the SM-only hypothesis is estimated by calculating $p_{\text{SM}}(q \leq q_{\text{obs}})$ for each M_{jj} bin separately. The largest difference is found in the M_{jj} range 3.0–3.6 TeV with a probability of 17% to obtain a deviation from the SM-only hypothesis larger than the observed, corresponding to a significance of 1.4 standard deviations. Including the two highest M_{jj} bins in the likelihood reduces this significance to 0.9 standard deviations, corresponding to a probability of 39%.

A modified-frequentist approach [52–54] is used to set exclusion limits on the scale Λ. Limits on the SM+NP models are set based on the quantity $\text{CL}_{\text{s}} = p_{\text{SM+NP}}(q \geq q_{\text{obs}})/(1 - p_{\text{SM}}(q \leq q_{\text{obs}}))$, which is required to be 0.05 for a 95% confidence level (CL) exclusion. The observed and expected exclusion limits on different CI and ADD models obtained in this analysis at 95% CL are listed in Tables 2 and 3 respectively. Note that the CI predictions with exact NLO QCD corrections show a smaller enhancement at low χ_{dijet} relative to QCD than do the corresponding LO

CI predictions, as described in detail in Ref. [55], and therefore result in less stringent limits.

Table 2: Observed and expected exclusion limits at 95% CL for various CI models. The uncertainties in the expected limits considering statistical and systematic effects for the SM-only hypothesis are also given.

Model	Observed (TeV)	Expected (TeV)
$\Lambda^{+}_{LL/RR}$ (LO)	10.3	9.8 ± 1.0
$\Lambda^{-}_{LL/RR}$ (LO)	12.9	12.4 ± 2.2
$\Lambda^{+}_{LL/RR}$ (NLO)	9.0	8.7 ± 0.8
$\Lambda^{-}_{LL/RR}$ (NLO)	11.7	11.4 ± 1.8
Λ^{+}_{VV} (NLO)	11.3	10.8 ± 1.1
Λ^{-}_{VV} (NLO)	15.2	14.6 ± 2.6
Λ^{+}_{AA} (NLO)	11.4	10.9 ± 1.1
Λ^{-}_{AA} (NLO)	15.1	14.5 ± 2.6
$\Lambda^{+}_{(V-A)}$ (NLO)	8.8	8.5 ± 1.1
$\Lambda^{-}_{(V-A)}$ (NLO)	8.9	8.6 ± 1.2

Table 3: Observed and expected exclusion limits at 95% CL for various ADD models in LO. The uncertainties in the expected limits considering statistical and systematic effects for the SM-only hypothesis are also given.

Model	Observed (TeV)	Expected (TeV)
ADD Λ_T (GRW)	7.1	6.8 ± 0.5
ADD M_S (HLZ) $n_{\mathrm{ED}} = 2$	6.9	6.6 ± 0.4
ADD M_S (HLZ) $n_{\mathrm{ED}} = 3$	8.4	8.0 ± 0.6
ADD M_S (HLZ) $n_{\mathrm{ED}} = 4$	7.1	6.8 ± 0.5
ADD M_S (HLZ) $n_{\mathrm{ED}} = 5$	6.4	6.1 ± 0.5
ADD M_S (HLZ) $n_{\mathrm{ED}} = 6$	5.9	5.7 ± 0.4

These results are also summarized in Fig. 3. The limits on M_S for the different n_{ED} ($n_{\mathrm{ED}} \geq 2$) directly follow from the limit for Λ_T. As a cross check, the limits for the CI scale $\Lambda^{+}_{LL/RR}$ are also determined for the case in which the data are not corrected for detector effects and instead the simulation predictions are convoluted with the detector resolutions. The extracted limits are found to agree with the quoted ones within 1%. We also quantify the effect of the inclusion of EW corrections in the QCD prediction on the $\Lambda^{+}_{LL/RR}$ (LO) observed limit, which would be reduced from 10.3 TeV to 9.8 TeV if EW corrections were neglected.

6 Summary

Normalized dijet angular distributions have been measured with the CMS detector over a wide range of dijet invariant masses. No significant deviation from the standard model predictions is observed. Lower limits are set on the contact interaction scale for a variety of quark compositeness models that include NLO QCD corrections and on the cutoff scale for the ADD models with extra dimensions. The 95% confidence level lower limits on the contact interaction scale Λ are in the range 8.8–15.2 TeV. The improved description of the data resulting from the inclusion of the electroweak corrections yields approximately 5% higher limits. The lower limits on the cutoff scales in the ADD models, Λ_T (GRW) and M_S (HLZ), are in the range 5.9–8.4 TeV. These

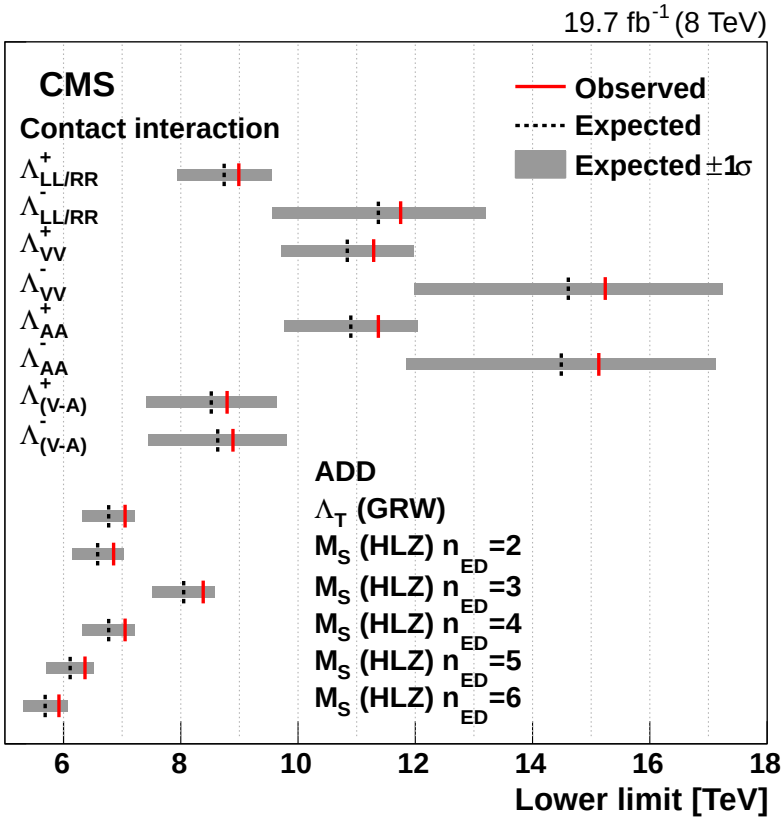

Figure 3: Observed (solid lines) and expected (dashed lines) 95% CL lower limits for the CI scales Λ for different compositeness models (NLO), for the ADD model scale with GRW parameterization Λ_T and for the ADD model scale with HLZ parameterization M_S. The gray bands indicate the corresponding uncertainties in the expected exclusion limits.

results represent the most stringent set of limits on contact interaction scale, modelled at NLO, and the best limits on the benchmark ADD model to date.

Acknowledgments

We would like to thank S. Dittmaier and A. Huss for providing us with the electroweak correction factors. We congratulate our colleagues in the CERN accelerator departments for the excellent performance of the LHC and thank the technical and administrative staffs at CERN and at other CMS institutes for their contributions to the success of the CMS effort. In addition, we gratefully acknowledge the computing centers and personnel of the Worldwide LHC Computing Grid for delivering so effectively the computing infrastructure essential to our analyses. Finally, we acknowledge the enduring support for the construction and operation of the LHC and the CMS detector provided by the following funding agencies: BMWFW and FWF (Austria); FNRS and FWO (Belgium); CNPq, CAPES, FAPERJ, and FAPESP (Brazil); MES (Bulgaria); CERN; CAS, MoST, and NSFC (China); COLCIENCIAS (Colombia); MSES and CSF (Croatia); RPF (Cyprus); MoER, ERC IUT and ERDF (Estonia); Academy of Finland, MEC, and HIP (Finland); CEA and CNRS/IN2P3 (France); BMBF, DFG, and HGF (Germany); GSRT (Greece); OTKA and NIH (Hungary); DAE and DST (India); IPM (Iran); SFI (Ireland); INFN (Italy); MSIP and NRF (Republic of Korea); LAS (Lithuania); MOE and UM (Malaysia); CINVESTAV, CONACYT, SEP, and UASLP-FAI (Mexico); MBIE (New Zealand); PAEC (Pakistan); MSHE and NSC (Poland); FCT (Portugal); JINR (Dubna); MON, RosAtom, RAS and RFBR (Russia); MESTD (Serbia); SEIDI and CPAN (Spain); Swiss Funding Agencies (Switzerland); MST (Taipei); ThEPCenter, IPST, STAR and NSTDA (Thailand); TUBITAK and TAEK (Turkey); NASU and SFFR (Ukraine); STFC (United Kingdom); DOE and NSF (USA).

References

[1] UA1 Collaboration, "Angular distributions for high-mass jet pairs and a limit on the energy scale of compositeness for quarks from the CERN $p\bar{p}$ collider", *Phys. Lett. B* **177** (1986) 244, doi:10.1016/0370-2693(86)91065-8.

[2] O. Klein, "Quantum theory and five-dimensional theory of relativity", *Z. Phys.* **37** (1926) 895, doi:10.1007/BF01397481.

[3] H. Terazawa, "Subquark model of leptons and quarks", *Phys. Rev. D* **22** (1980) 184–199, doi:10.1103/PhysRevD.22.184.

[4] E. Eichten, K. D. Lane, and M. E. Peskin, "New Tests for Quark and Lepton Substructure", *Phys. Rev. Lett.* **50** (1983) 811, doi:10.1103/PhysRevLett.50.811.

[5] E. Eichten, I. Hinchliffe, K. D. Lane, and C. Quigg, "Super Collider Physics", *Rev. Mod. Phys.* **56** (1984) 579, doi:10.1103/RevModPhys.56.579.

[6] CDF Collaboration, "Measurement of Dijet Angular Distributions by the Collider Detector at Fermilab", *Phys. Rev. Lett.* **77** (1996) 5336, doi:10.1103/PhysRevLett.77.5336, arXiv:hep-ex/9609011. [Erratum doi:10.1103/RevModPhys.58.1065].

[7] D0 Collaboration, "Measurement of dijet angular distributions at $\sqrt{s} = 1.96$ TeV and searches for quark compositeness and extra spatial dimensions", *Phys. Rev. Lett.* **103** (2009) 191803, doi:10.1103/PhysRevLett.103.191803, arXiv:0906.4819.

[8] D0 Collaboration, "High-p_{T} jets in $\bar{p}p$ collisions at $\sqrt{s} = 630$ GeV and 1800 GeV", *Phys. Rev. D* **64** (2001) 032003, doi:10.1103/PhysRevD.64.032003, arXiv:hep-ex/0012046.

[9] CMS Collaboration, "Search for quark compositeness in dijet angular distributions from pp collisions at $\sqrt{s} = 7$ TeV", *J. High Energy Phys.* **05** (2012) 055, doi:10.1007/JHEP05(2012)055.

[10] CMS Collaboration, "Measurement of Dijet Angular Distributions and Search for Quark Compositeness in pp Collisions at $\sqrt{s} = 7$ TeV", *Phys. Rev. Lett.* **106** (2011) 201804, doi:10.1103/PhysRevLett.106.201804.

[11] CMS Collaboration, "Search for Quark Compositeness with the Dijet Centrality Ratio in pp Collisions at $\sqrt{s}$ = 7 TeV", *Phys. Rev. Lett.* **105** (2010) 262001, doi:10.1103/PhysRevLett.105.262001.

[12] ATLAS Collaboration, "ATLAS search for new phenomena in dijet mass and angular distributions using pp collisions at $\sqrt{s} = 7$ TeV", *JHEP* **01** (2013) 029, doi:10.1007/JHEP01(2013)029, arXiv:1210.1718.

[13] ATLAS Collaboration, "Search for New Physics in Dijet Mass and Angular Distributions in pp Collisions at $\sqrt{s} = 7$ TeV Measured with the ATLAS Detector", *New J. Phys.* **13** (2011) 053044, doi:10.1088/1367-2630/13/5/053044, arXiv:1103.3864.

[14] CMS Collaboration, "Search for contact interactions using the inclusive jet p_{T} spectrum in pp collisions at $\sqrt{s} = 7$ TeV", *Phys. Rev. D* **87** (2013) 052017, doi:10.1103/PhysRevD.87.052017.

[15] N. Arkani-Hamed, S. Dimopoulos, and G. Dvali, "Phenomenology, astrophysics and cosmology of theories with submillimeter dimensions and TeV scale quantum gravity", *Phys. Rev. D* **59** (1999) 086004, doi:10.1103/PhysRevD.59.086004, arXiv:hep-ph/9807344.

[16] N. Arkani-Hamed, S. Dimopoulos, and G. Dvali, "The hierarchy problem and new dimensions at a millimeter", *Phys. Lett. B* **429** (1998) 263, doi:10.1016/S0370-2693(98)00466-3, arXiv:hep-ph/9803315.

[17] G. F. Giudice, R. Rattazzi, and J. D. Wells, "Quantum gravity and extra dimensions at high-energy colliders", *Nucl. Phys. B* **544** (1999) 3, doi:10.1016/S0550-3213(99)00044-9.

[18] T. Han, J. D. Lykken, and R. Zhang, "Kaluza-Klein states from large extra dimensions", *Phys. Rev. D* **59** (1999) 105006, doi:10.1103/PhysRevD.59.105006.

[19] J. Hewett, "Indirect collider signals for extra dimensions", *Phys. Rev. Lett.* **82** (1999) 4765, doi:10.1103/PhysRevLett.82.4765.

[20] K. Cheung and G. Landsberg, "Drell-Yan and Diphoton production at hadron colliders and low scale gravity model", *Phys. Rev. D* **62** (2000) 076003, doi:10.1103/PhysRevD.62.076003, arXiv:hep-ph/9909218.

[21] CMS Collaboration, "Search for physics beyond the standard model in dilepton mass spectra in proton-proton collisions at $\sqrt{s} = 8$ TeV", (2014). arXiv:1412.6302. Submitted to JHEP.

[22] ATLAS Collaboration, "Search for contact interactions and large extra dimensions in the dilepton channel using proton-proton collisions at $\sqrt{s} = 8$ TeV with the ATLAS detector", *Eur. Phys. J. C* **74** (2014) 314, doi:10.1140/epjc/s10052-014-3134-6, arXiv:1407.2410.

[23] CMS Collaboration, "Search for signatures of extra dimensions in the diphoton mass spectrum at the Large Hadron Collider", *Phys. Rev. Lett.* **108** (2011) 111801, doi:10.1103/PhysRevLett.108.111801.

[24] ATLAS Collaboration, "Search for extra dimensions in diphoton events using proton-proton collisions recorded at $\sqrt{s} = 7$ TeV with the ATLAS detector at the LHC", *New J. Phys.* **15** (2013) 043007, doi:10.1088/1367-2630/15/4/043007, arXiv:1210.8389.

[25] ATLAS Collaboration, "Search for quark contact interactions in dijet angular distributions in pp collisions at $\sqrt{s} = 7$ TeV measured with the ATLAS detector", *Phys. Lett. B* **694** (2011) 327, doi:10.1016/j.physletb.2010.10.021, arXiv:1009.5069.

[26] R. Franceschini et al., "LHC bounds on large extra dimensions", *JHEP* **05** (2011) 092, doi:10.1007/JHEP05(2011)092, arXiv:1101.4919.

[27] CMS Collaboration, "The CMS experiment at the CERN LHC", *JINST* **3** (2008) S08004, doi:10.1088/1748-0221/3/08/S08004.

[28] CMS Collaboration, "Particle–Flow Event Reconstruction in CMS and Performance for Jets, Taus, and $E_{\mathrm{T}}^{\mathrm{miss}}$", CMS Physics Analysis Summary CMS-PAS-PFT-09-001, 2009.

[29] CMS Collaboration, "Commissioning of the Particle-flow Event Reconstruction with the first LHC collisions recorded in the CMS detector", CMS Physics Analysis Summary CMS-PAS-PFT-10-001, 2010.

[30] M. Cacciari, G. P. Salam, and G. Soyez, "The anti-k_t jet clustering algorithm", *JHEP* **04** (2008) 063, doi:10.1088/1126-6708/2008/04/063, arXiv:0802.1189.

[31] M. Cacciari, G. P. Salam, and G. Soyez, "FastJet user manual", *Eur. Phys. J. C* **72** (2012) 1896, doi:10.1140/epjc/s10052-012-1896-2, arXiv:1111.6097.

[32] CMS Collaboration, "Determination of jet energy calibration and transverse momentum resolution in CMS", *J. Instrum.* **6** (2011) P11002, doi:10.1088/1748-0221/6/11/P11002.

[33] CMS Collaboration, "Jets in 0.9 and 2.36 TeV pp Collisions", CMS Physics Analysis Summary CMS-PAS-JME-10-001, 2010.

[34] G. d'Agostini, "A multidimensional unfolding method based on Bayes' theorem", *Nucl. Instrum. Meth. A* **362** (1995) 487, doi:10.1016/0168-9002(95)00274-X.

[35] T. Adye, "Unfolding algorithms and tests using RooUnfold", in *Proceedings of the PHYSTAT 2011 Workshop on Statistical Issues Related to Discovery Claims in Search Experiments and Unfolding*, p. 313. CERN, Geneva, Switzerland, January 17-20, 2011. arXiv:1105.1160. doi:10.5170/CERN-2011-006.

[36] S. Gieseke et al., "Herwig++ 2.5 release note", (2011). arXiv:1102.1672.

[37] M. Bähr et al., "Herwig++ physics and manual", *Eur. Phys. J. C* **58** (2008) 639, doi:10.1140/epjc/s10052-008-0798-9, arXiv:0803.0883.

[38] M. J. Oreglia, "A study of the reactions $\psi' \to \gamma\gamma\psi$". PhD thesis, Stanford University, 1980. SLAC Report SLAC-R-236, see Appendix D.

[39] CMS Collaboration, "8 TeV jet energy corrections and uncertainties based on 19.8 fb^{-1} of data in CMS", CMS Detector Performance Summary DP-2013-033, 2013.

[40] GEANT4 Collaboration, "GEANT4—a simulation toolkit", *Nucl. Instrum. Meth. A* **506** (2003) 250, doi:10.1016/S0168-9002(03)01368-8.

[41] T. Sjöstrand, S. Mrenna, and P. Z. Skands, "A Brief Introduction to PYTHIA 8.1", *Comput. Phys. Commun.* **178** (2008) 852, doi:10.1016/j.cpc.2008.01.036, arXiv:0710.3820.

[42] R. Corke and T. Sjöstrand, "Interleaved parton showers and tuning prospects", *JHEP* **03** (2011) 032, doi:10.1007/JHEP03(2011)032, arXiv:1011.1759.

[43] CMS Collaboration, "Measurement of the inelastic proton-proton cross section at $\sqrt{s} = 7\,\text{TeV}$", *Phys. Lett. B* **722** (2013) 5, doi:10.1016/j.physletb.2013.03.024.

[44] Z. Nagy, "Three jet cross-sections in hadron hadron collisions at next-to-leading order", *Phys. Rev. Lett.* **88** (2002) 122003, doi:10.1103/PhysRevLett.88.122003, arXiv:hep-ph/0110315.

[45] Z. Nagy, "Next-to-leading order calculation of three jet observables in hadron hadron collision", *Phys. Rev. D* **68** (2003) 094002, doi:10.1103/PhysRevD.68.094002, arXiv:hep-ph/0307268.

[46] T. Kluge, K. Rabbertz, and M. Wobisch, "fastNLO: Fast pQCD calculations for PDF fits", in *14th International Workshop on Deep-Inelastic Scattering (DIS 2006)*, p. 483. Tsukuba, Japan, Apr 20-24, April, 2006. arXiv:hep-ph/0609285. doi:10.1142/9789812706706_0110.

[47] D. Britzger, K. Rabbertz, F. Stober, and M. Wobisch, "New features in version 2 of the fastNLO project", in *20th International Workshop on Deep-Inelastic Scattering and Related Subjects (DIS 2012)*, p. 217. Bonn, Germany, March 26-30, 2012. arXiv:1208.3641. doi:10.3204/DESY-PROC-2012-02/165.

[48] S. Dittmaier, A. Huss, and C. Speckner, "Weak radiative corrections to dijet production at hadron colliders", *JHEP* **11** (2012) 095, doi:10.1007/JHEP11(2012)095, arXiv:1210.0438.

[49] A. Banfi, G. P. Salam, and G. Zanderighi, "Phenomenology of event shapes at hadron colliders", *JHEP* **06** (2010) 038, doi:10.1007/JHEP06(2010)038.

[50] H.-L. Lai et al., "New parton distributions for collider physics", *Phys. Rev. D* **82** (2010) 074024, doi:10.1103/PhysRevD.82.074024, arXiv:1007.2241.

[51] J. Gao et al., "Next-to-leading QCD effect to the quark compositeness search at the LHC", *Phys. Rev. Lett.* **106** (2011) 142001, doi:10.1103/PhysRevLett.106.142001, arXiv:1101.4611.

[52] R. D. Cousins and V. L. Highland, "Incorporating systematic uncertainties into an upper limit", *Nucl. Instrum. Meth. A* **320** (1992) 331, doi:10.1016/0168-9002(92)90794-5.

[53] T. Junk, "Confidence level computation for combining searches with small statistics", *Nucl. Instrum. Meth. A* **434** (1999) 435, doi:10.1016/s0168-9002(99)00498-2, arXiv:hep-ph/9811356.

[54] A. L. Read, "Presentation of search results: the CL_s technique", *J. Phys. G* **28** (2002) 2693, doi:10.1088/0954-3899/28/10/313.

[55] J. Gao, C. S. Li, and C. P. Yuan, "NLO QCD corrections to dijet production via quark contact interactions", *JHEP* **07** (2012) 037, doi:10.1007/JHEP07(2012)037, arXiv:1204.4773.

A EW corrections to dijet angular distributions

Figure 4 shows the EW corrections to the dijet angular distributions. The corrections are based on the same calculations and tools used to derive the EW corrections to inclusive jet and dijet production cross sections published in Ref. [48]. The authors of Ref. [48] have provided the exact numbers to be applied to the dijet angular distribution as presented in this paper. The EW corrections change the predictions of the normalized χ_{dijet} distributions by up to 4% (14%) at low (high) M_{jj}.

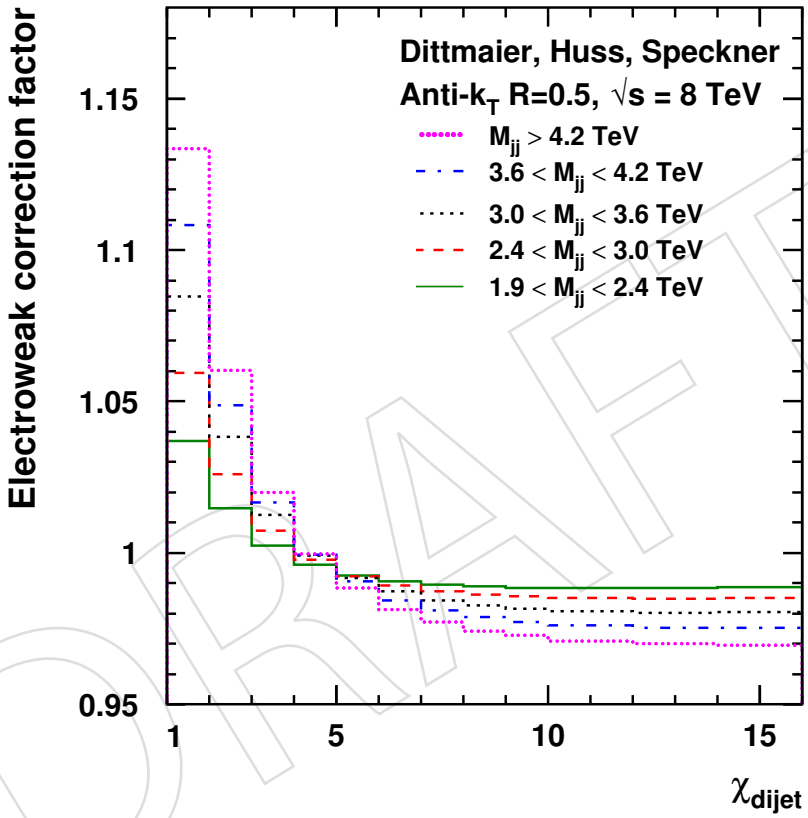

Figure 4: Electroweak correction factors versus χ_{dijet} for each M_{jj} range, derived by the authors of Ref. [48] at 8 TeV c.m. energy with $\langle p_{\text{T1,2}} \rangle$ as choice for the μ_R and μ_F scales and the CT10-NLO PDF set.